Contribution to the benchmark proposal of Hans Kuerten: LES of particle-laden channel flow.

Simulations of Christian Gobert, TU Munich

January 27, 2010

1 Overview and description of the simulations

This document contains statistics corresponding to the statistics presented in Marchioli *et al.* [1]. The statistics are shown in (almost) the same order as in Marchioli *et al.* [1]. The data shown is from DNS, LES and semi-DNS, i.e., a simulation on the LES grid without LES model. The simulations were performed by Hans Kuerten (TU Eindhoven, TUE) and Christian Gobert & Michael Manhart (TU Munich, TUM). Table 1 gives some details on the TUM-simulations. Furthermore, in the TUM-simulations

- all grids are streched grids, i.e., finer close to the wall than at the channel center. The grids are shown in figure 1
- for LES, the dynamic Lagrange Smagorinsky model proposed by Meneveau *et al.* [2] was implemented
- the (filtered) Navier–Stokes equations were discretized by a second order Finite-Volume method
- for time advancement of the fluid flow, a third order Runge–Kutta method was implemented
- the particle velocity was integrated in time using a 4th order adaptive linear-implicit Runge–Kutta scheme (Rosenbrock–Wanner scheme)
- interpolation of fluid velocity on particles' position is trilinear or fourth order. For fourth order interpolation close to the wall, a non-symmetric stencil (with respect to the particle position) was chosen, i.e., close to the wall, the interpolation is based on the three points which are nearest to the wall and the wall itself where $u = v = w = 0$
- in accordance with the simulations of Hans Kuerten, the particle statistics were averaged from $t^+ = 0$ to $t^+ = 16000$
- for computing particle statistics, the benchmark-binning was implemented, the bins defined by

$$y_j = Re_\tau \frac{\tanh\left(\Delta\left(j_{max} - j\right)/j_{max}\right)}{\tanh\Delta}, \qquad \Delta = 1.7, \quad j_{max} = 96$$

  The reader is reminded that the binning for sampling particle statistics does not coincide with the grid for the fluid flow.
- all particle-related quantities are plotted at the y^+-value that corresponds to the upper boundary of the corresponding bin, i.e., the statistics of particles which are located between y_j and y_{j+1} are plotted at y_{j+1}.

2 Some comments on the results

The following contains some comments on the results from sections 3, 4 and 5.

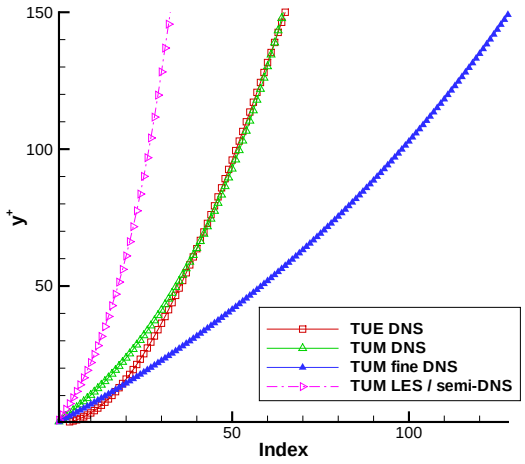

Figure 1: Grid spacing in the wall-normal direction

Table 1: Overview on the simulations

label	number of grid points	distance of first grid point to the wall	interpolation of fluid velocity seen by particles
DNS	128^3 (benchmark resolution)	$y^+ = 1$	trilinear
fine DNS	256^3	$y^+ = 0.7$	n.a.(fluid statistics only)
LES trilin	64^3 (benchmark resolution)	$y^+ = 2$	trilinear
LES 4thO.	64^3 (benchmark resolution)	$y^+ = 2$	4th order
semi-DNS trilin	64^3 (benchmark resolution)	$y^+ = 2$	trilinear
semi-DNS 4thO.	64^3 (benchmark resolution)	$y^+ = 2$	4th order

2.1 Comments on the fluid statistics

Figures 2 to 6 show statistics on the fluid phase. Apparently the TUM DNS shows smaller rms values than the two reference DNS. This was to be expected because the TUM DNS is based on a second order Finite Volume scheme and shows therefore higher numerical dissipation that the UUD DNS and the TUE DNS which are both based on spectral methods. This hypothesis is supported by the fact that the TUM DNS on the fine grid is closer to the spectral solutions than the TUM DNS on the standard grid.
Concerning the LES result, it is remarkable that the dynamic Lagrangian Smagorinsky model leads to an overestimation of the mean velocity and rms of velocity fluctuations in the streamwise direction but an underestimation of the rms values in spanwise and wall-normal direction. However, this behavior is well known, see [2]. The results from the semi-DNS are as expected.
Concerning the streamwise/wall-normal component of the Reynolds stress, all DNS and even the semi-DNS agree very well with each other. The LES underpredicts that quantity (refering to its absolute value).
The shown fluid statistics are these which are presented in Marchioli *et al.* [1]. As requested by the benchmark specification, more statistics up to fourth order were computed. Concerning these statistics, good agreement between TUM DNS and TUE DNS was observed concerning second order statistics. Skewness and flatness seems to be predicted uncorrectly by TUM DNS, probably due to the low order of the scheme.

2.2 Comments on the particle statistics

Concerning particle statistics, Marchioli *et al.* [1] show the temporal development of particle concentration close to the wall. This quantity depends on the binning. In the present work, the binning is different to the binning used by Marchioli *et al.*. Therefore, results on the concentration at the wall from the present work are not one-to-one comparable to the results presented by Marchioli *et al.*.
However, figures 7 to 9 show the temporal development of particle concentration near the wall. For $St = 1$ and $St = 5$, this is the concentration below $y^+ = 0.36$. The $St = 25$-particles have a diameter of $0.765y^*$. Therefore these particles do not get closer to the wall than $y^+ = 0.38$. Consequently, figure 9 shows the concentration below $y^+ = 0.73$ for $St = 25$.
Figures 7 to 9 show that in LES and semi-DNS, the particle concentration near the wall depends heavily

on interpolation. For $St = 1$ and $St = 5$, fourth order interpolation leads to too low concentrations next to the wall in LES and semi-DNS, compared against the DNS result. However, this does not mean that LES or semi-DNS with fourth order interpolation does not predict turbophoresis, see below. The reader is reminded that for $St = 1$ and $St = 5$, figures 7 and 8 show the particles in $y^+ < 0.36$ whereas for $St = 25$, figure 9 shows the particles in $y^+ < 0.73$. Thus, figure 9 is not fully comparable to figures 7 and 8.
The particle concentration at the channel center is shown as a function of time in figures 10 to 12. Figures 7 to 12 show that the time for obtaining a statistically state is independent of interpolation and equal in DNS, LES and semi-DNS.
Figures 13 to 15 show time-averaged particle concentrations in the statistically steady state (from $t^+ = 16000$ to $t^+ = 20000$ after particle initialization). It was already observed before that for $St = 1$ and $St = 5$, the fourth order interpolation leads to too low particle concentrations near the wall in LES or semi-DNS. Figures 13 and 14 indicate that the concentration maximum tends to be closer to the channel center with fourth order interpolation than with trilinear interpolation. The shift is more pronounced on the coarser grid. Even with the rather compact Hermite interpolation, conducted by Hans Kuerten, TUE, such a shift can be observed, cf. also figures 31 and 32.
In all TUM-results presented in figures 13, 31 and 32, the concentration seems to show a slight increase around the first grid point. This issue is discussed below.
The mean streamwise particle velocites are shown in figures 16 to 18. The deviations of LES or semi-DNS to DNS are a consequence of the deviations observed for the fluid phase, cf. figure 2. The same holds for the rms values, figures 19 to 27.
The particle Reynolds stress differs significantly in DNS / LES or semi-DNS, cf. figures 28 to 30. This was not observed for the fluid Reynolds stress, cf. figure 6. The TUM DNS and the TUE DNS are in good agreement concerning the fluid Reynolds stress and particle Reynolds stress for $St = 1$ and $St = 5$ but for $St = 25$, these two DNS show different results on the particle Reynolds stress. However, similar observations were already found by Marchioli *et al.* [1]. In that paper, several codes showed good agreement in fluid Reynolds stress but not so good agreement in particle Reynolds stress. In general, particle Reynolds stress seems to be underpredicted (refering to the absolute value) by LES or, even stronger, by semi-DNS.

2.3 Comments on the comparison of TUE and TUM results

Figures 31 to 36 show time averaged particle concentration profiles from the TUE and the TUM simulations. As mentioned above, these results seem to indicate that the grid might affect the concentration profile, even in DNS. The effect is most pronounced for $St = 1$. There seems to be an increase in concentration around the first grid point, i.e., the grid point cloest to the wall. The reader is reminded that for TUM DNS, the first grid point is at $y^+ = 1$, for TUM LES and TUM semi-DNS at $y^+ = 2$, for TUE DNS at $y^+ = 0.045$, for TUE LES and TUE semi-DNS at $y^+ = 0.18$. Thus, if the grid affects the concentration profiles, then this can only be observed in the TUM simulations. However, results on other grids might help to clarify that issue.
On the other hand, in most aspects the results from the TUM and TUE simulations agree with each other. Figures 31 to 36 indicate that turbophoresis is underpredicted by LES. Concerning semi-DNS, there seems to be no clear trend whether turbophoresis is under- or overpredicted. The effect of the interpolation scheme is unclear for $St = 1$. For $St = 5$ or $St = 25$, higher order interpolation leads to better results in LES or semi-DNS than trilinear interpolation.
Concerning average and rms values of particle velocity, the differences between the TUE and the TUM simulations are mostly due to the different accuracy of the flow solvers. Moreover, the differences between semi-DNS, LES and DNS concerning average and rms values of particle velocity are a consequence of the differences which were already observed in the fluid statistics. The average streamwise particle velocity seems to be underpredicted by semi-DNS but overpredicted by LES, cf. figures 37 to 42. The effect is stronger in the TUM LES than in the TUE LES. The effect of interpolation is negligible.
Concerning rms values of particle velocity (figures 43 to 60), for the streamwise component, semi-DNS leads to an underprediction but LES to an overprediction. Concerning spanwise and wall-normal components, semi-DNS and LES lead to an underprediction. Fourth order interpolation always leads to higher values than trilinear interpolation. The effects are stronger in the TUM simulations than in the TUE simulations.
The streamwise/wall-normal component of the particle-Reynolds stress (figures 61-66) is in general underpredicted by semi-DNS or LES (with respect to absolute values). However, the differences are very small in the TUE fourth order simulations.
The largest difference between TUE and TUM results is in the concentration profiles for $St = 5$ with semi-DNS (figure 33). The TUE results indicate that semi-DNS leads to an overprediction of turbophoresis for $St = 5$ whereas the TUM results indicate that semi-DNS leads to an underprediction of turbophoresis. The effect seems to be stronger with with the higher order interpolation.

3 Fluid statistics

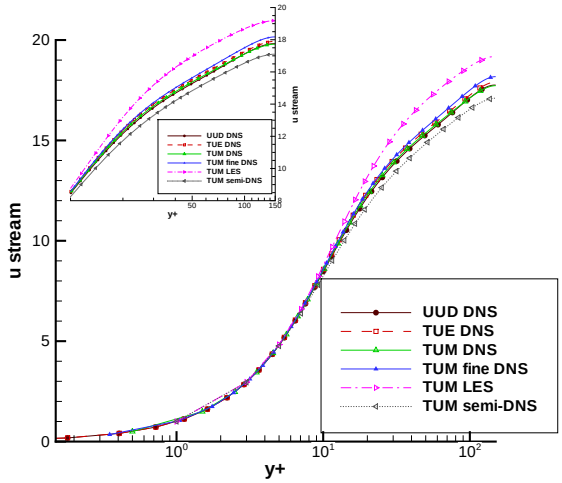

Figure 2: Mean streamwise fluid velocity

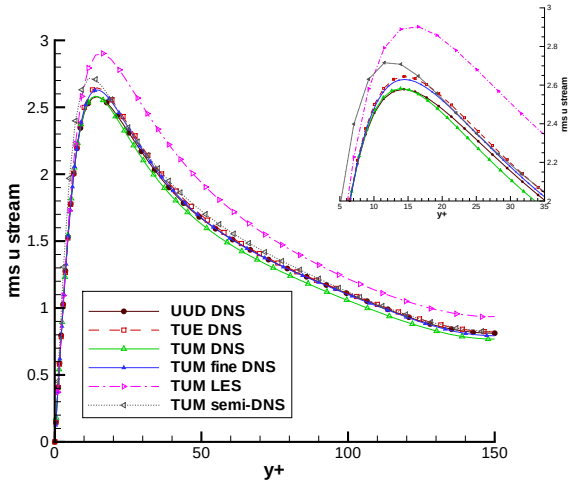

Figure 3: rms of fluid velocity fluctuations (streamwise)

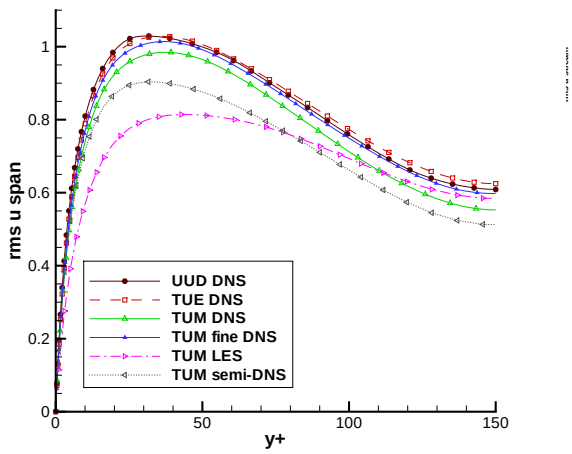

Figure 4: rms of fluid velocity fluctuations (spanwise)

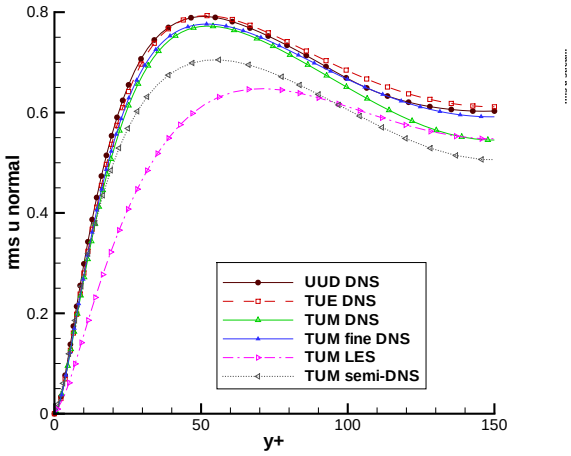

Figure 5: rms of fluid velocity fluctuations (wall-normal)

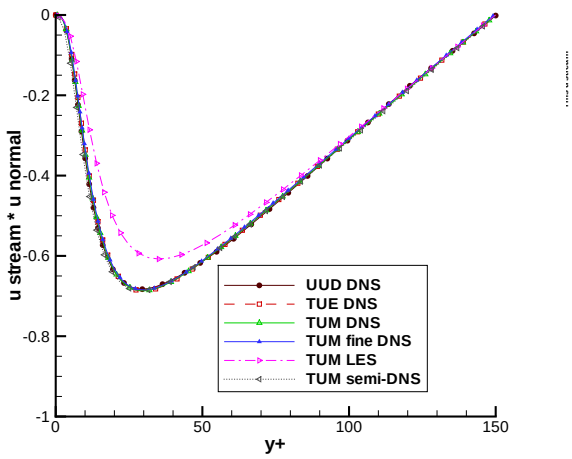

Figure 6: Fluid Reynolds stress: streamwise/wall-normal component

4 Particle statistics

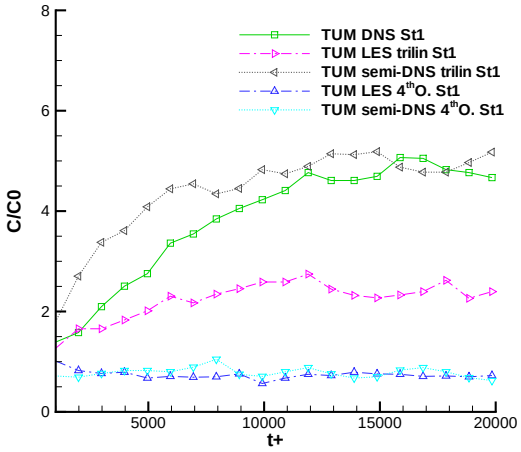

Figure 7: Particle concentration close to the wall (below $y^+ = 0.36$) as function of time, $St = 1$

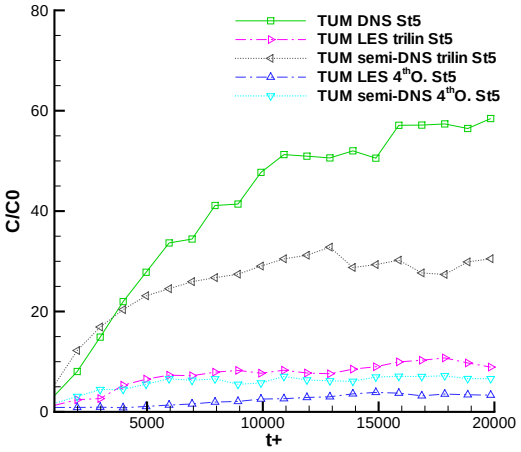

Figure 8: Particle concentration close to the wall (below $y^+ = 0.36$) as function of time, $St = 5$

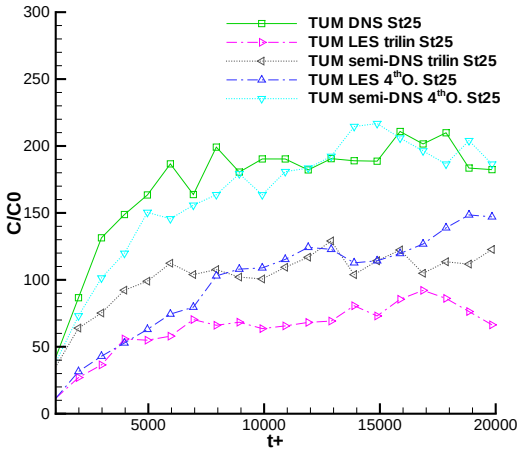

Figure 9: Particle concentration close to the wall (below $y^+ = 0.73$) as function of time, $St = 25$

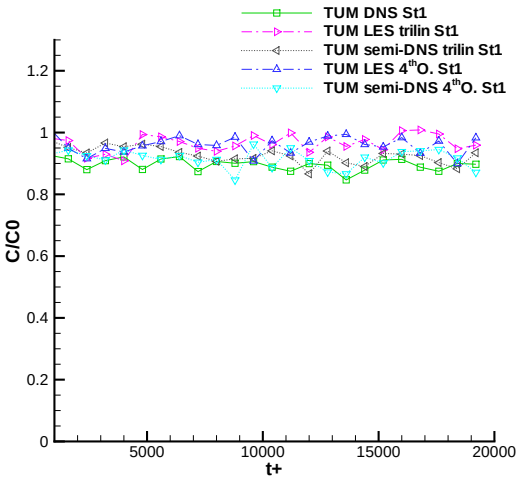

Figure 10: Particle concentration at the center as function of time, $St = 1$

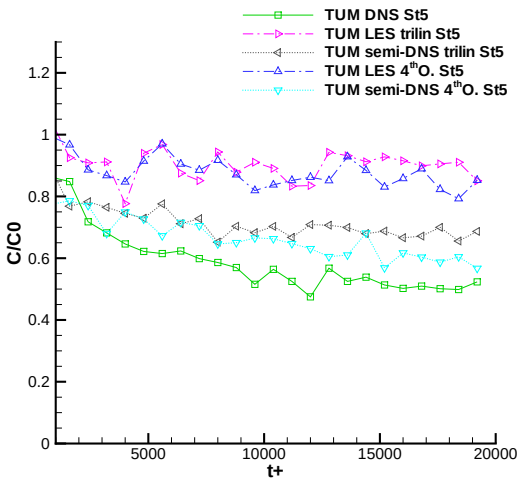

Figure 11: Particle concentration at the center as function of time, $St = 5$

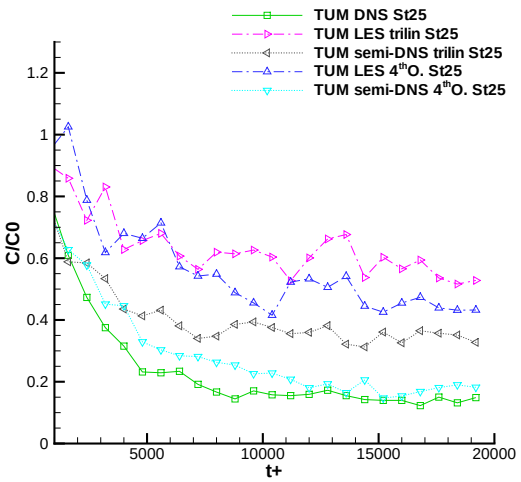

Figure 12: Particle concentration at the center as function of time, $St = 25$

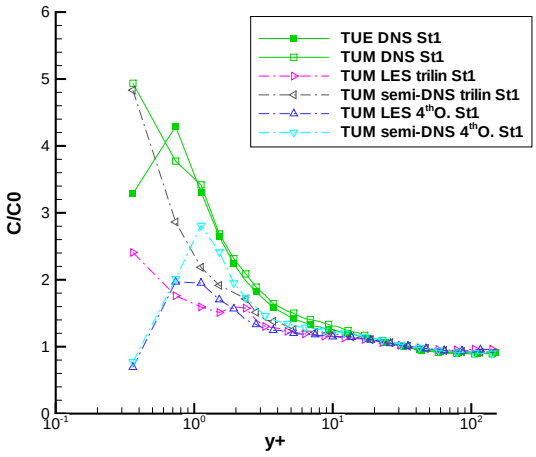

Figure 13: Time-averaged particle concentration profile between $t^+ = 16000$ and $t^+ = 20000$, $St = 1$.

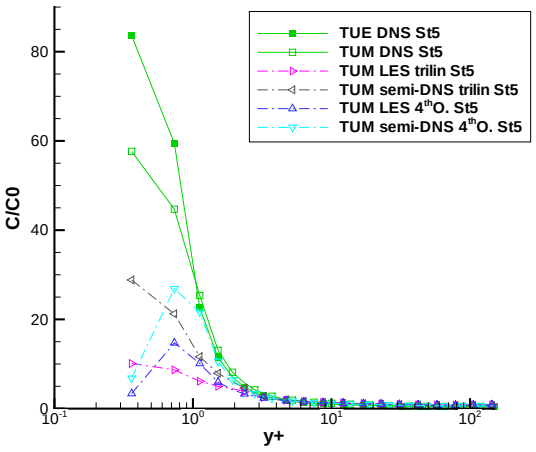

Figure 14: Time-averaged particle concentration profile between $t^+ = 16000$ and $t^+ = 20000$, $St = 5$.

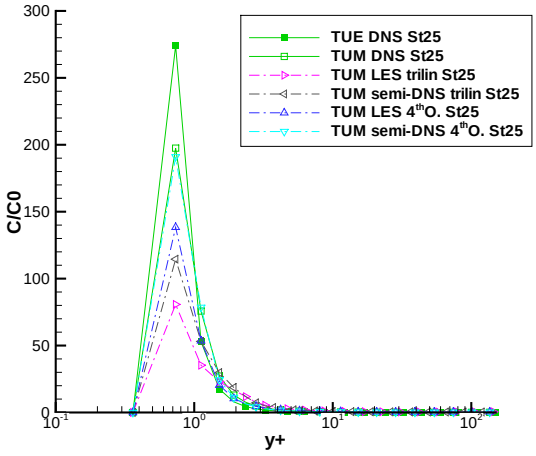

Figure 15: Time-averaged particle concentration profile between $t^+ = 16000$ and $t^+ = 20000$, $St = 25$.

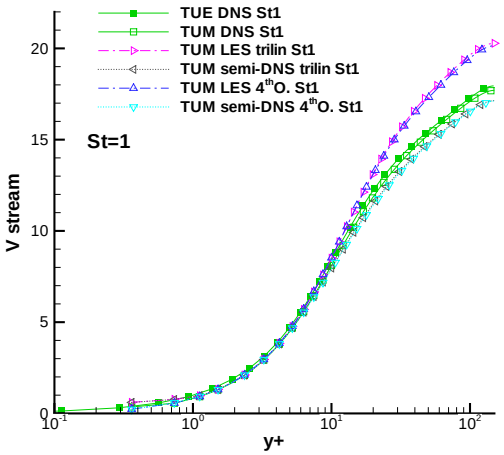

Figure 16: Average streamwise particle velocity, $St = 1$

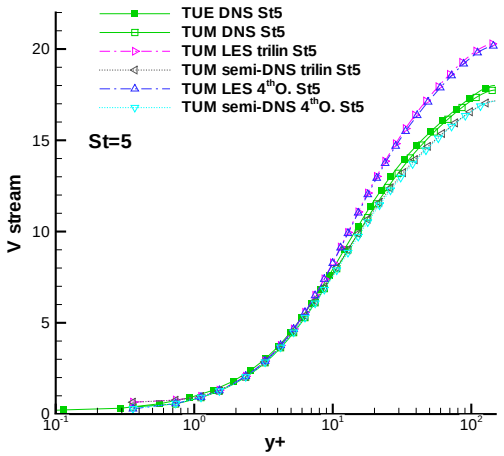

Figure 17: Average streamwise particle velocity, $St = 5$

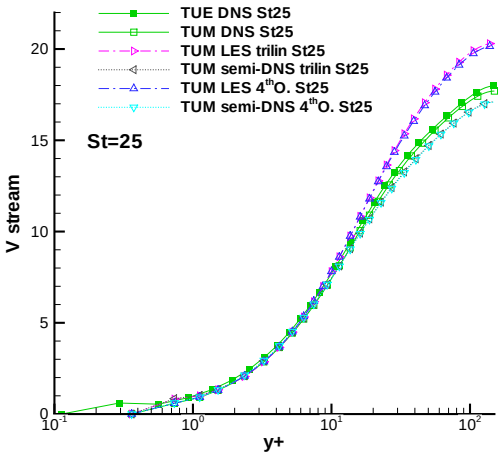

Figure 18: Average streamwise particle velocity, $St = 25$

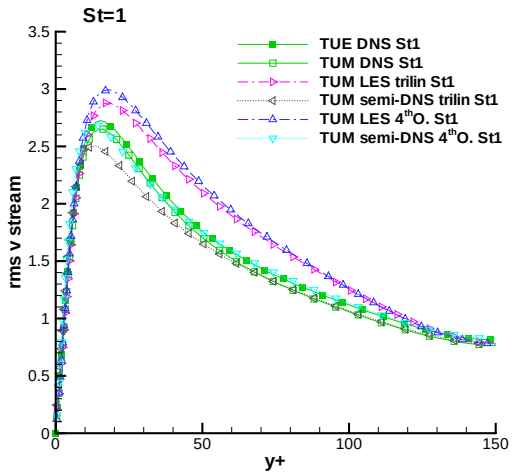

Figure 19: rms of particle streamwise velocity fluctuations, $St = 1$

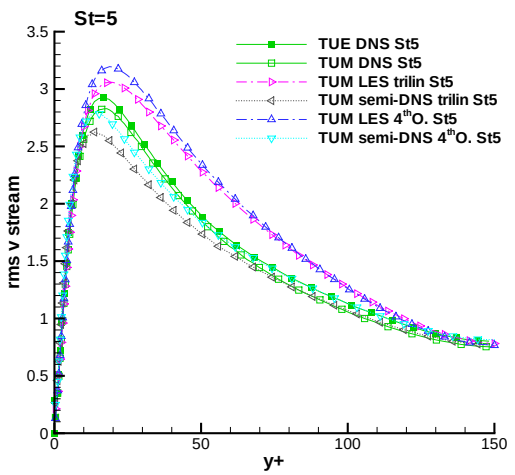

Figure 20: rms of particle streamwise velocity fluctuations, $St = 5$

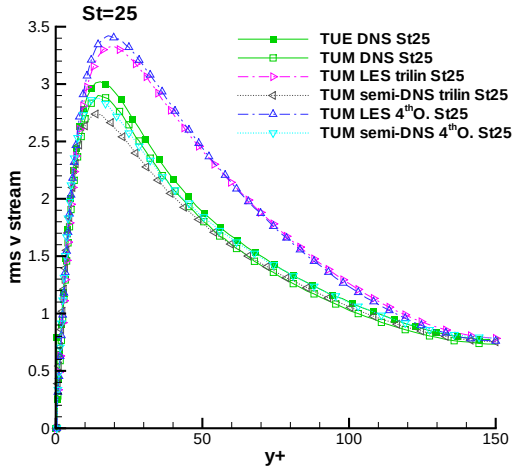

Figure 21: rms of particle streamwise velocity fluctuations, $St = 25$

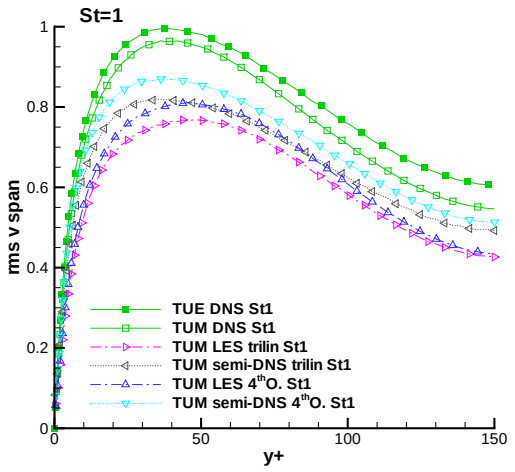

Figure 22: rms of particle spanwise velocity fluctuations, $St = 1$

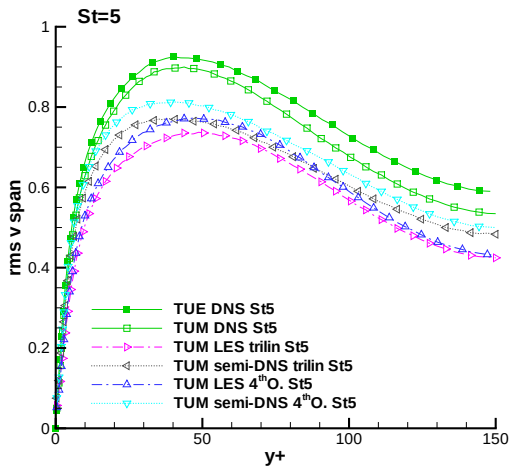

Figure 23: rms of particle spanwise velocity fluctuations, $St = 5$

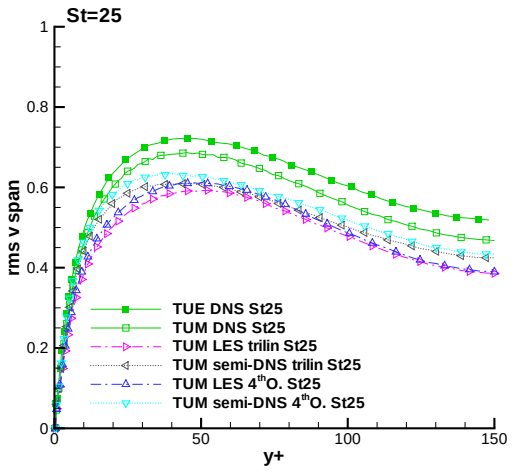

Figure 24: rms of particle spanwise velocity fluctuations, $St = 25$

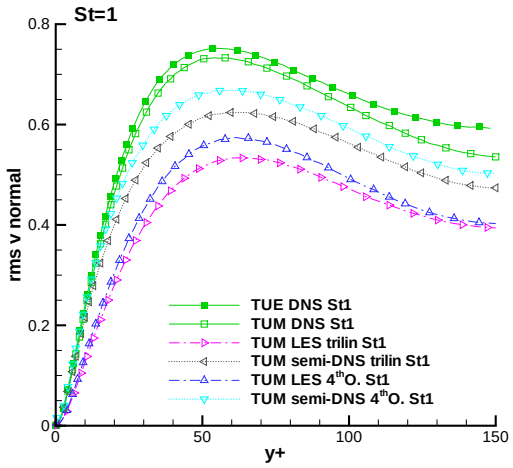

Figure 25: rms of particle wall-normal velocity fluctuations, $St = 1$

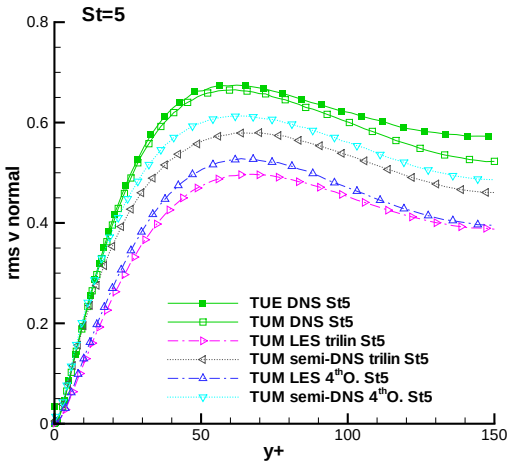

Figure 26: rms of particle wall-normal velocity fluctuations, $St = 5$

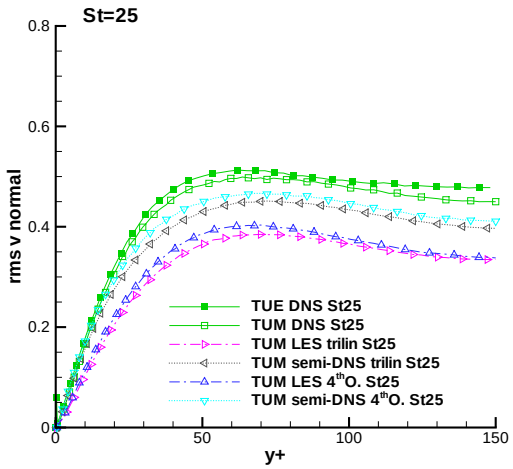

Figure 27: rms of particle wall-normal velocity fluctuations, $St = 25$

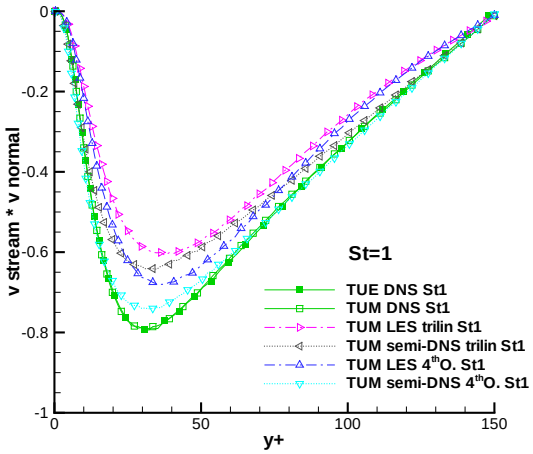

Figure 28: particle Reynolds stresses, streamwise/wall-normal component, $St = 1$

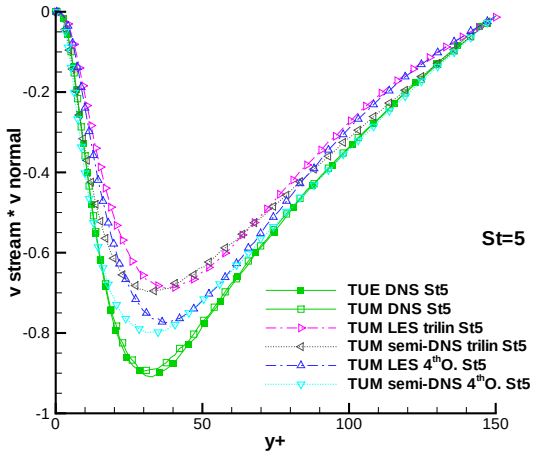

Figure 29: particle Reynolds stresses, streamwise/wall-normal component, $St = 5$

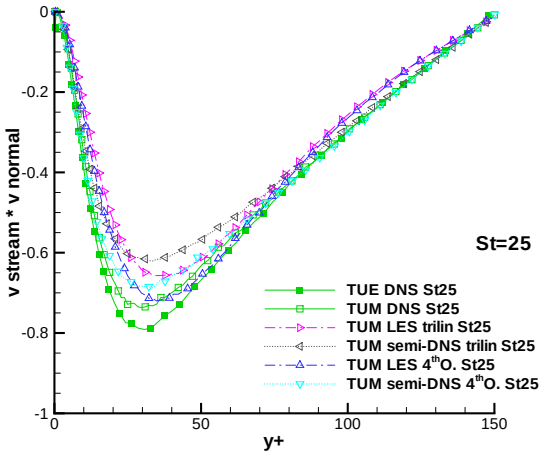

Figure 30: particle Reynolds stresses, streamwise/wall-normal component, $St = 25$

5 Comparison TUE-TUM

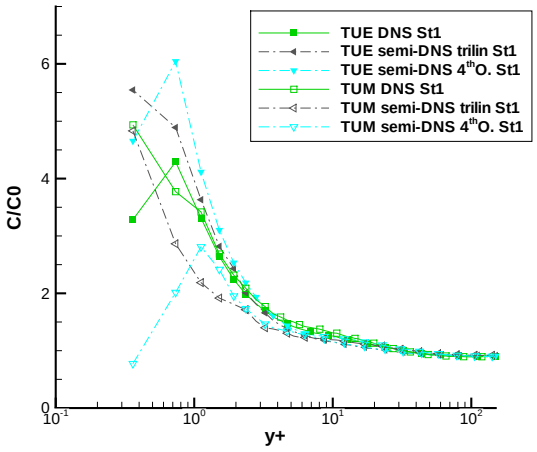

Figure 31: Time-averaged particle concentration profile between $t^+ = 16000$ and $t^+ = 20000$, $St = 1$.

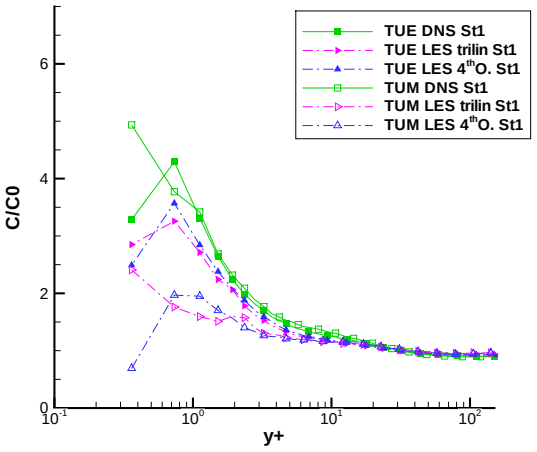

Figure 32: Time-averaged particle concentration profile between $t^+ = 16000$ and $t^+ = 20000$, $St = 1$.

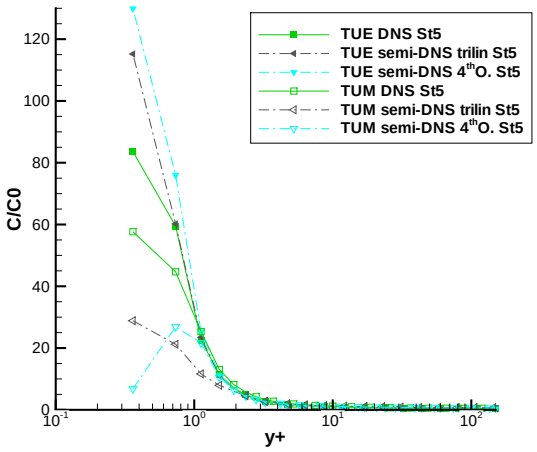

Figure 33: Time-averaged particle concentration profile between $t^+ = 16000$ and $t^+ = 20000$, $St = 5$.

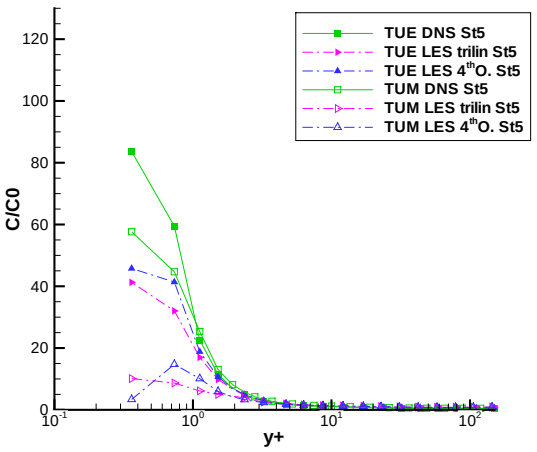

Figure 34: Time-averaged particle concentration profile between $t^+ = 16000$ and $t^+ = 20000$, $St = 5$.

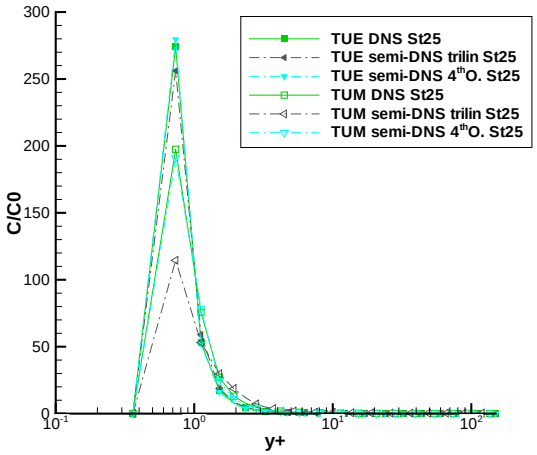

Figure 35: Time-averaged particle concentration profile between $t^+ = 16000$ and $t^+ = 20000$, $St = 25$.

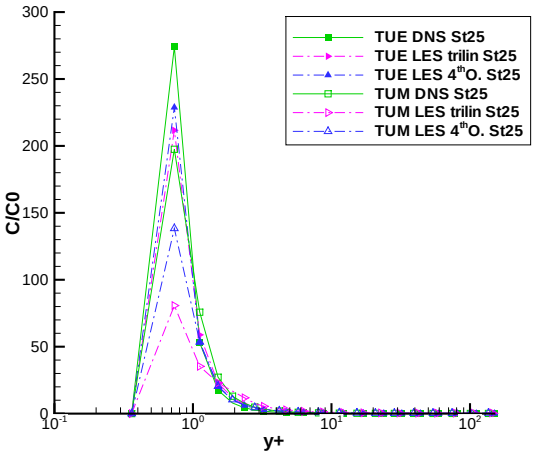

Figure 36: Time-averaged particle concentration profile between $t^+ = 16000$ and $t^+ = 20000$, $St = 25$.

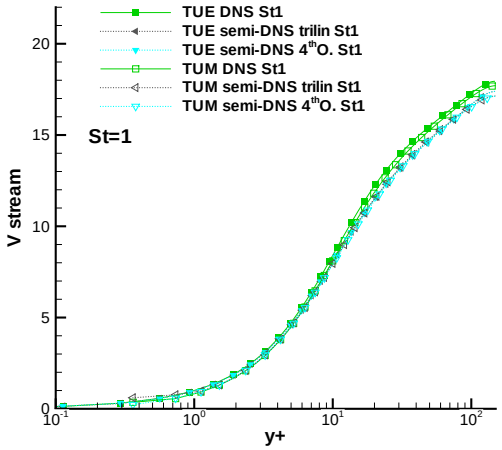

Figure 37: Average streamwise particle velocity, $St = 1$

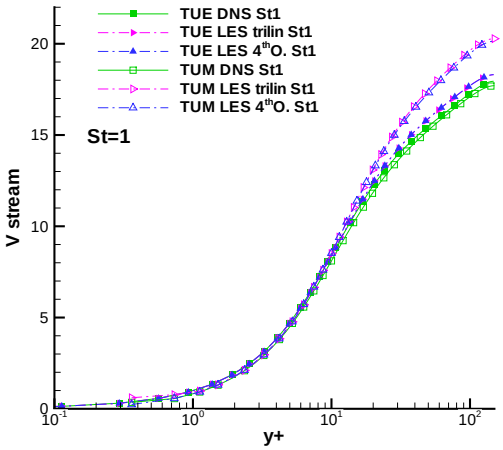

Figure 38: Average streamwise particle velocity, $St = 1$

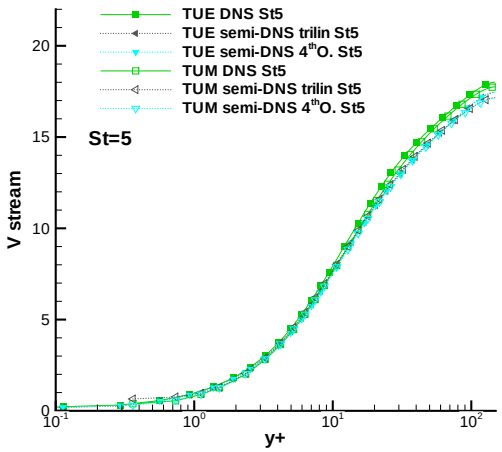

Figure 39: Average streamwise particle velocity, $St = 5$

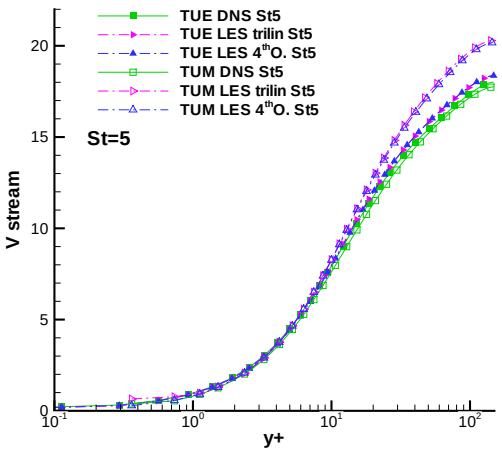

Figure 40: Average streamwise particle velocity, $St = 5$

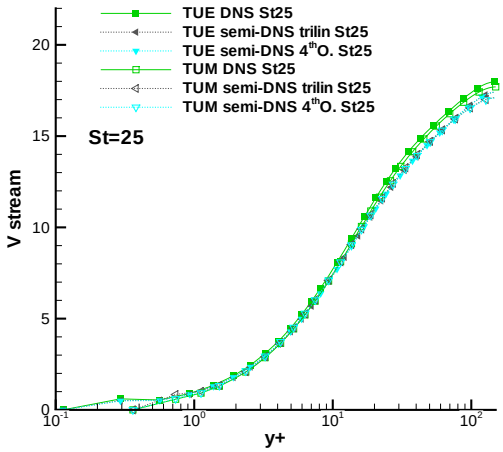

Figure 41: Average streamwise particle velocity, $St = 25$

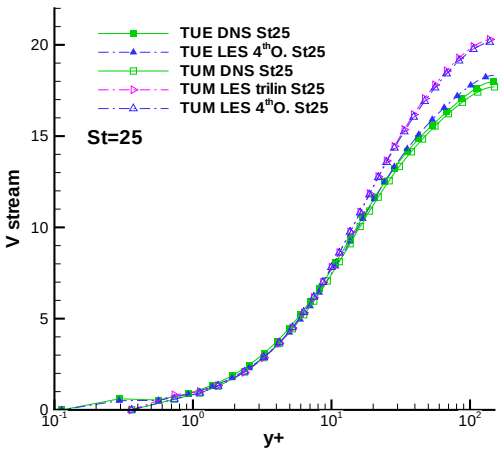

Figure 42: Average streamwise particle velocity, $St = 25$

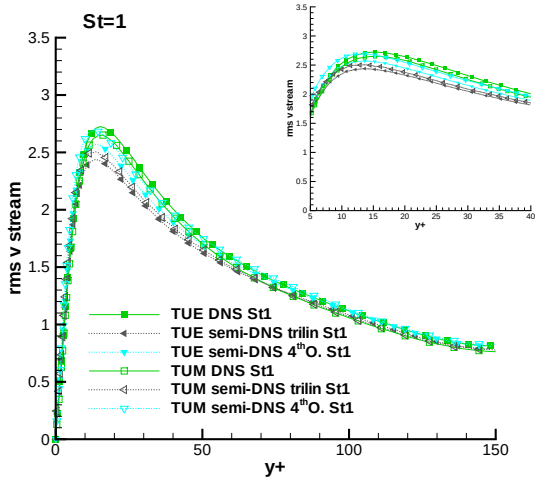

Figure 43: rms of particle streamwise velocity fluctuations, $St = 1$

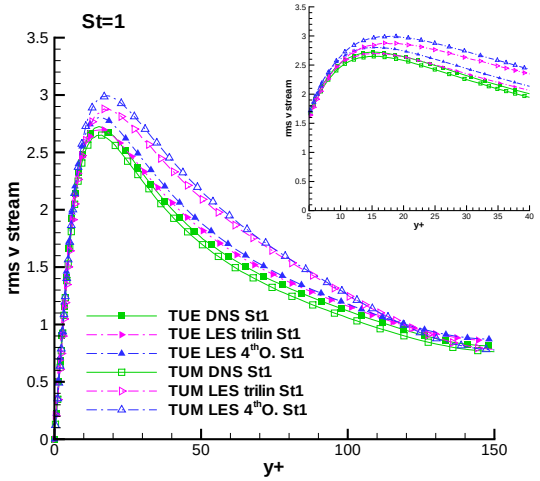

Figure 44: rms of particle streamwise velocity fluctuations, $St = 1$

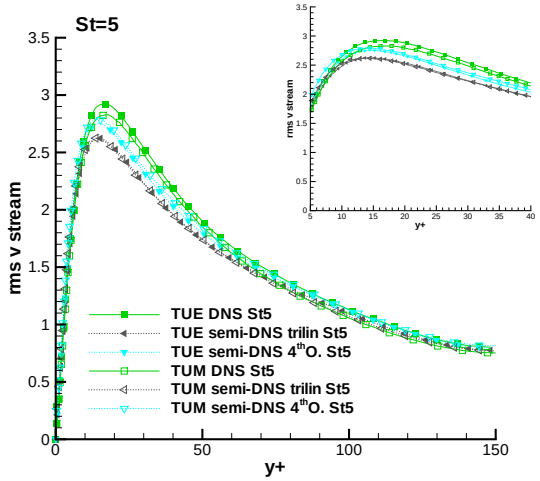

Figure 45: rms of particle streamwise velocity fluctuations, $St = 5$

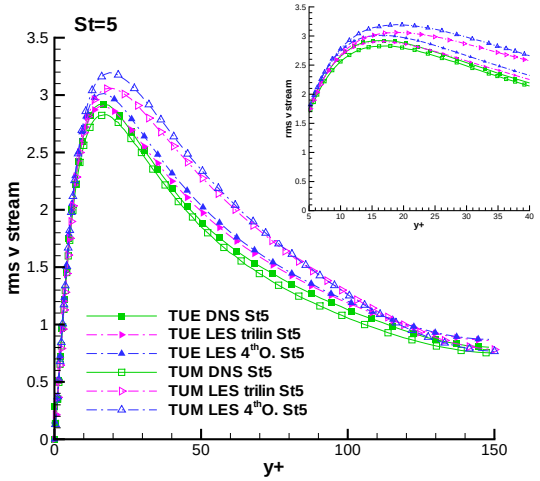

Figure 46: rms of particle streamwise velocity fluctuations, $St = 5$

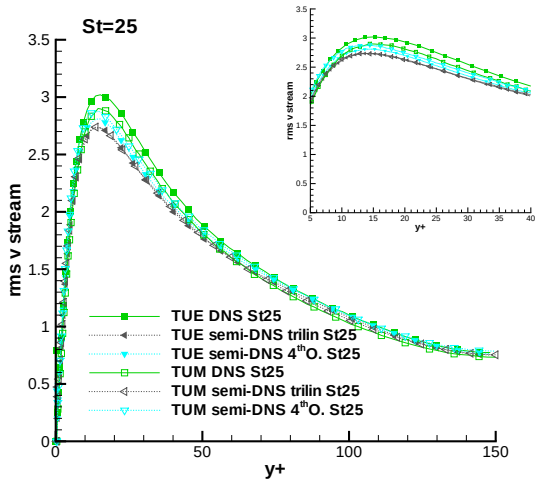

Figure 47: rms of particle streamwise velocity fluctuations, $St = 25$

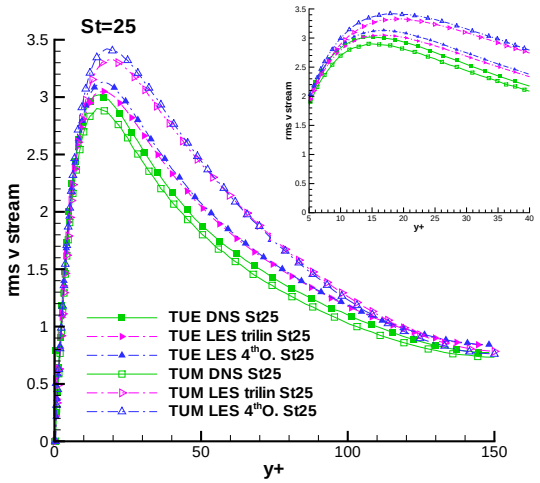

Figure 48: rms of particle streamwise velocity fluctuations, $St = 25$

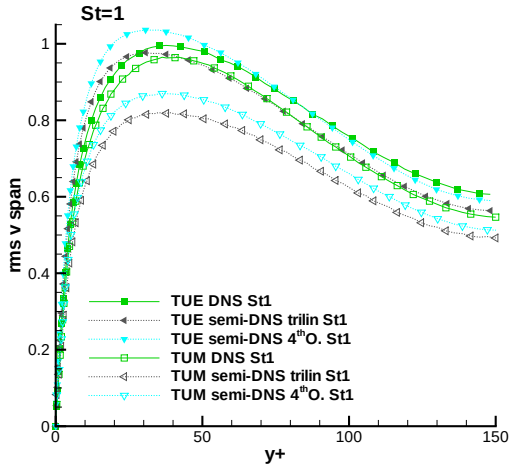

Figure 49: rms of particle spanwise velocity fluctuations, $St = 1$

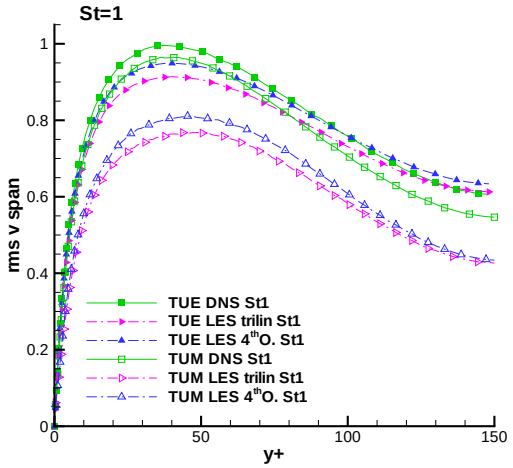

Figure 50: rms of particle spanwise velocity fluctuations, $St = 1$

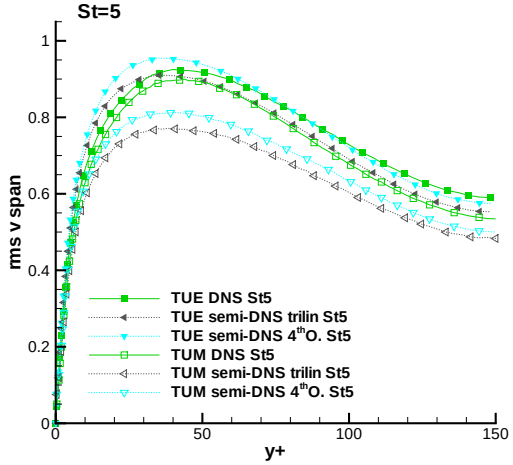

Figure 51: rms of particle spanwise velocity fluctuations, $St = 5$

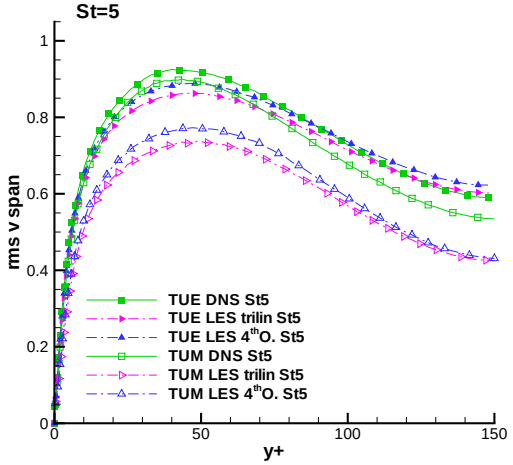

Figure 52: rms of particle spanwise velocity fluctuations, $St = 5$

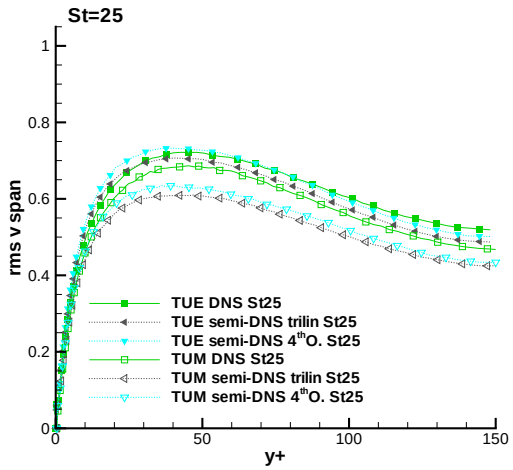

Figure 53: rms of particle spanwise velocity fluctuations, $St = 25$

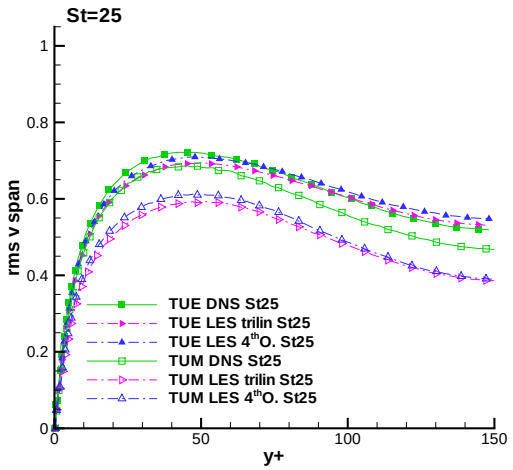

Figure 54: rms of particle spanwise velocity fluctuations, $St = 25$

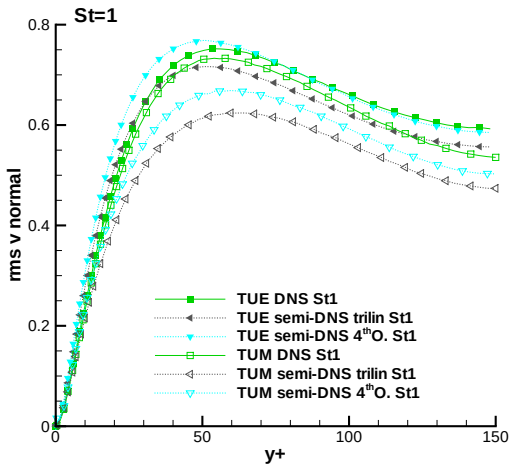

Figure 55: rms of particle wall-normal velocity fluctuations, $St = 1$

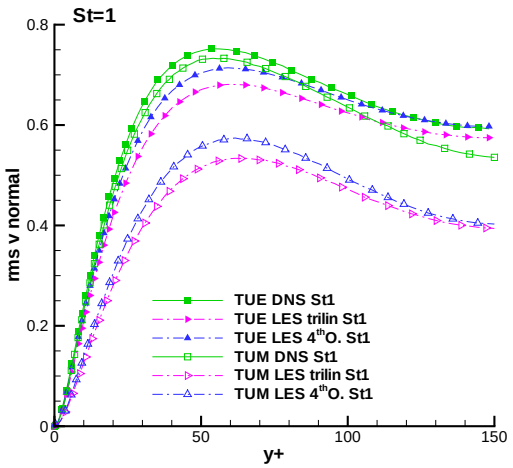

Figure 56: rms of particle wall-normal velocity fluctuations, $St = 1$

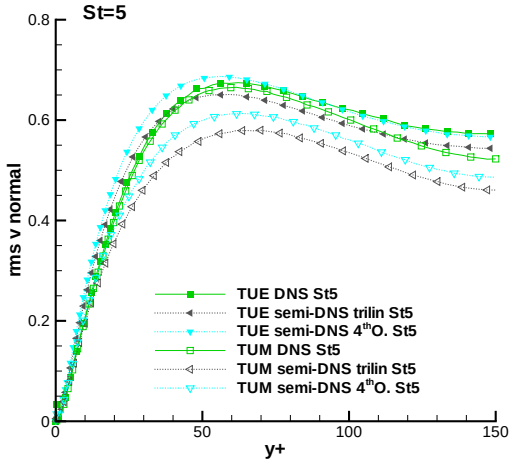

Figure 57: rms of particle wall-normal velocity fluctuations, $St = 5$

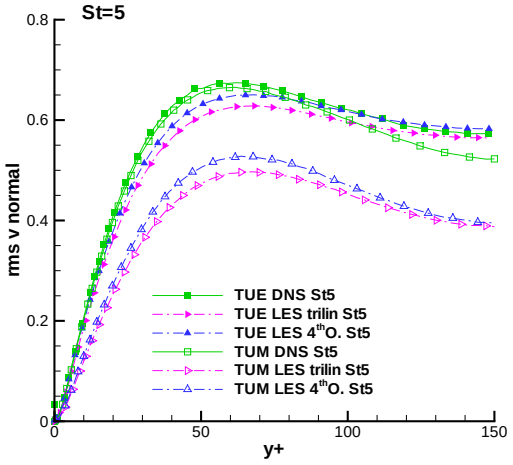

Figure 58: rms of particle wall-normal velocity fluctuations, $St = 5$

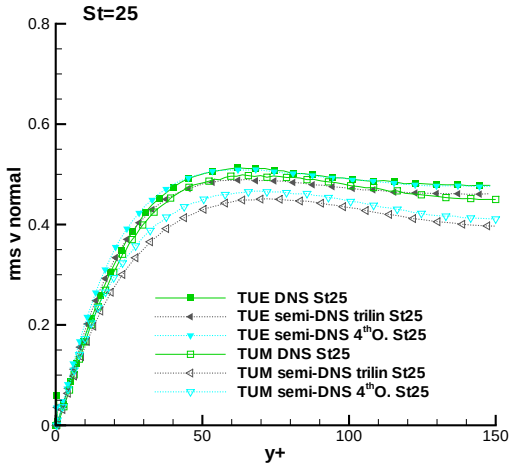

Figure 59: rms of particle wall-normal velocity fluctuations, $St = 25$

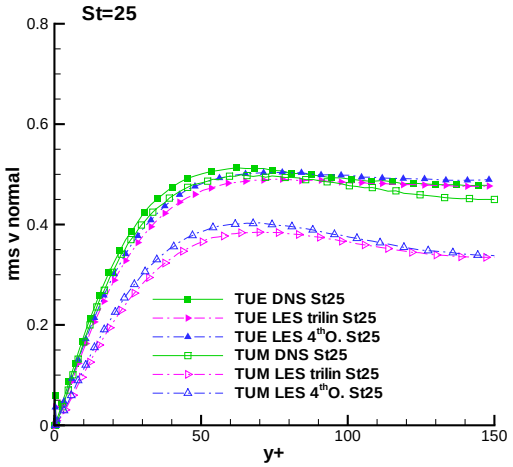

Figure 60: rms of particle wall-normal velocity fluctuations, $St = 25$

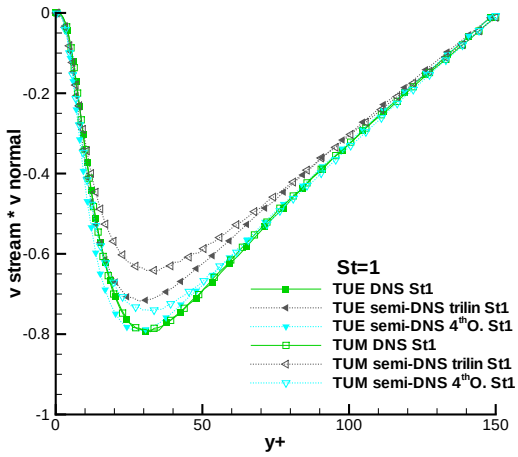

Figure 61: particle Reynolds stresses, streamwise/wall-normal component, $St = 1$

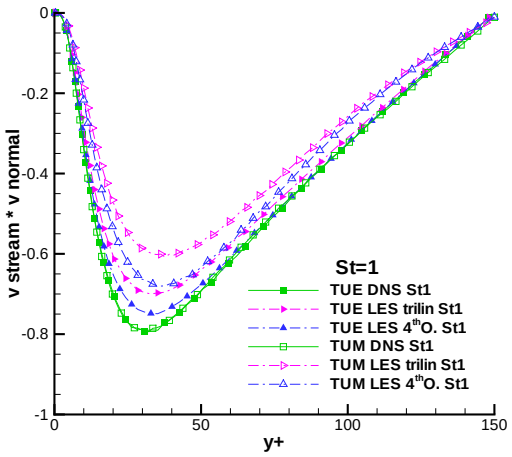

Figure 62: particle Reynolds stresses, streamwise/wall-normal component, $St = 1$

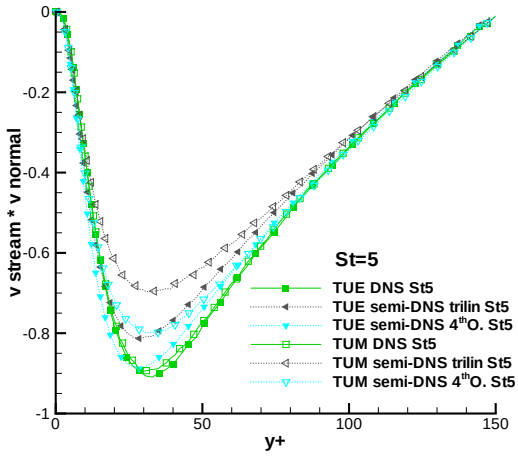

Figure 63: particle Reynolds stresses, streamwise/wall-normal component, $St = 5$

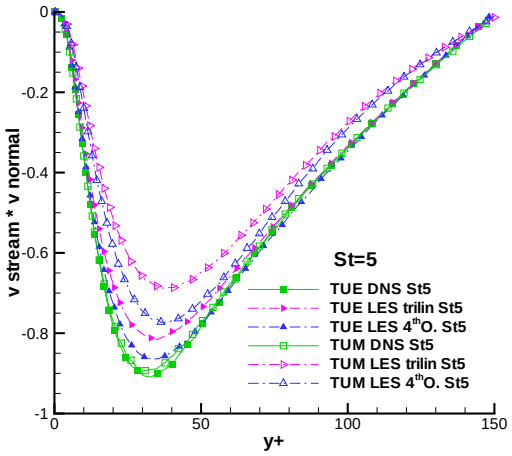

Figure 64: particle Reynolds stresses, streamwise/wall-normal component, $St = 5$

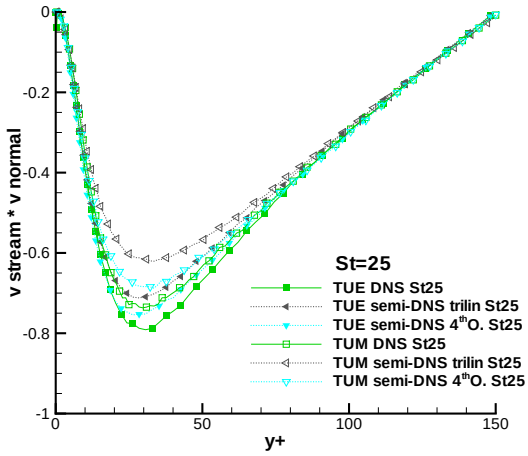

Figure 65: particle Reynolds stresses, streamwise/wall-normal component, $St = 25$

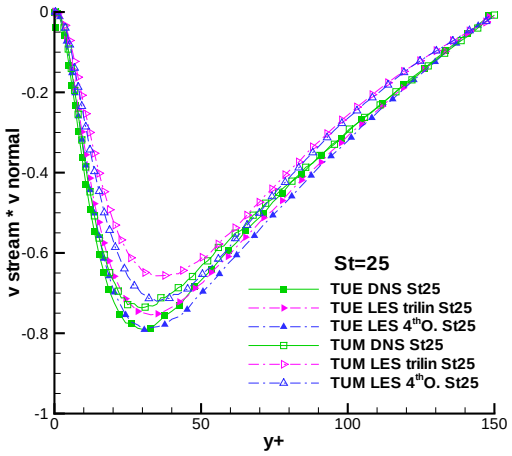

Figure 66: particle Reynolds stresses, streamwise/wall-normal component, $St = 25$

6 Index of figures / data

Figure	file	data columns
2	dns_results, finedns_results, les_results, semidns_results	1,2
3	dns_results, finedns_results, les_results, semidns_results	1,4
4	dns_results, finedns_results, les_results, semidns_results	1,6
5	dns_results, finedns_results, les_results, semidns_results	1,5
6	dns_results, finedns_results, les_results, semidns_results	1,10
7	dns_concentration_wall, les2_concentration_wall, semidns2_concentration_wall, les4_concentration_wall, semidns4_concentration_wall	1,2
8	dns_concentration_wall, les2_concentration_wall, semidns2_concentration_wall, les4_concentration_wall, semidns4_concentration_wall	1,3
9	dns_concentration_wall, les2_concentration_wall, semidns2_concentration_wall, les4_concentration_wall, semidns4_concentration_wall	1,4
10	dns_concentration_center, les2_concentration_center, semidns2_concentration_center, les4_concentration_center, semidns4_concentration_center	1,2
11	dns_concentration_center, les2_concentration_center, semidns2_concentration_center, les4_concentration_center, semidns4_concentration_center	1,3
12	dns_concentration_center, les2_concentration_center, semidns2_concentration_center, les4_concentration_center, semidns4_concentration_center	1,4
13	dns_concentration, les2_concentration, semidns2_concentration, les4_concentration, semidns4_concentration	1,65
14	dns_concentration, les2_concentration, semidns2_concentration, les4_concentration, semidns4_concentration	1,66
15	dns_concentration, les2_concentration, semidns2_concentration, les4_concentration, semidns4_concentration	1,67
16	dns_particles_1, les2_particles_1, semidns2_particles_1, les4_particles_1, semidns4_particles_1	1,3
17	dns_particles_5, les2_particles_5, semidns2_particles_5, les4_particles_5, semidns4_particles_5	1,3
18	dns_particles_25, les2_particles_25, semidns2_particles_25, les4_particles_25, semidns4_particles_25	1,3
19	dns_particles_1, les2_particles_1, semidns2_particles_1, les4_particles_1, semidns4_particles_1	1,6
20	dns_particles_5, les2_particles_5, semidns2_particles_5, les4_particles_5, semidns4_particles_5	1,6
21	dns_particles_25, les2_particles_25, semidns2_particles_25, les4_particles_25, semidns4_particles_25	1,6
22	dns_particles_1, les2_particles_1, semidns2_particles_1, les4_particles_1, semidns4_particles_1	1,8
23	dns_particles_5, les2_particles_5, semidns2_particles_5, les4_particles_5, semidns4_particles_5	1,8
24	dns_particles_25, les2_particles_25, semidns2_particles_25, les4_particles_25, semidns4_particles_25	1,8

Figure	file	data columns
25	dns_particles_1, les2_particles_1, semidns2_particles_1, les4_particles_1, semidns4_particles_1	1,7
26	dns_particles_5, les2_particles_5, semidns2_particles_5, les4_particles_5, semidns4_particles_5	1,7
27	dns_particles_25, les2_particles_25, semidns2_particles_25, les4_particles_25, semidns4_particles_25	1,7
28	dns_particles_1, les2_particles_1, semidns2_particles_1, les4_particles_1, semidns4_particles_1	1,10
29	dns_particles_5, les2_particles_5, semidns2_particles_5, les4_particles_5, semidns4_particles_5	1,10
30	dns_particles_25, les2_particles_25, semidns2_particles_25, les4_particles_25, semidns4_particles_25	1,10

References

[1] Marchioli, C., Soldati, A., Kuerten, J., Arcen, B., Taniere, A., Goldensoph, G., Squires, K., Cargnelutti, M. & Portela, L. 2008 Statistics of particle dispersion in direct numerical simulations of wall-bounded turbulence: Results of an international collaborative benchmark test. *Int. J. Multiphase Flow* **34**, 879–893.

[2] Meneveau, C., Lund, T. S. & Cabot, W. H. 1996 A Lagrangian dynamic subgrid-scale model of turbulence. *J. Fluid Mech.* **319**, 353–385.